Pergamon

*Int. J. Solids Structures* Vol. 34, No. 16, pp. 2061–2072, 1997

0020-7683/97 $17.00 + .00

PII: S0020-7683(96)00138-2

# FINITE ELEMENT ANALYSIS OF WALL PRESSURE IN IMPERFECT SILOS

J. Y. OOI
Department of Civil Engineering, University of Edinburgh, Crew Building, The King's Buildings, Edinburgh EH9 3JL, U.K.

and

K. M. SHE
Department of Civil Engineering, University of Brighton, Cockcroft Building, Lewes Road, Brighton BN2 4GJ, U.K.

(*Received* 20 *October* 1995; *in revised form* 21 *June* 1996)

**Abstract**—It is generally accepted that the pressures exerted by stored bulk solid on silo walls after filling are closely predicted by the Janssen theory. However, recent experimental observations of silo wall pressure have shown significant deviations from Janssen pressures even after careful symmetrical filling. Both meridional and circumferential variations from the Janssen values have been found, which induce bending of the wall in reinforced concrete silos and high membrane stresses in steel silos. It has been suggested that the presence of geometric imperfections in the silo wall is a likely cause of these pressure variations. However, no rigorous investigation of the effects of uneven surface profile on wall pressures appears to have been performed, though some simple calculations have been produced. This paper presents a finite element study of the effects of a local axisymmetric wall imperfection on pressures acting on the wall of a circular silo. The effects of imperfection height and imperfection geometry on wall pressures are also investigated. © 1997 Elsevier Science Ltd.

## NOTATION

| | |
|---|---|
| $E_w$, $E_s$ | Young's modulus of silo wall and stored solid, respectively |
| $H$ | silo height |
| $P_p$ | peak pressure |
| $P_\infty$ | Janssen asymptotic normal wall pressure ($=\gamma R/2\mu$) |
| $R$ | silo radius |
| $t$ | silo wall thickness |
| $z$ | vertical coordinate with origin at silo floor |
| $z_o$ | vertical coordinate at centre of geometric imperfection |
| $\alpha$ | stiffness parameter ($=E_s R/E_w t$) |
| $\beta$ | angle of the conical surcharge of stored solid (angle of repose) |
| $\delta_o$ | amplitude of geometric imperfection |
| $\lambda$ | silo wall shell bending half wavelength ($=2.44\sqrt{Rt}$) |
| $\nu_w$, $\nu_s$ | Poisson's ratio of silo wall and stored solid, respectively |

## 1. INTRODUCTION

It is generally accepted that the silo wall pressures exerted by stored bulk solid after filling are closely predicted by the Janssen theory (1895). However, recent silo pressure experiments have shown that significant deviations from the Janssen pressure distribution can occur even under careful symmetrical filling (Munch-Andersen and Nielsen, 1990; Ooi *et al.*, 1990; Ooi and Rotter, 1991). In general, the departures from Janssen pressures vary in both the vertical and horizontal directions, and have been shown to be both large and systematically repeatable from one test to another in the same silo (Ooi *et al.*, 1990). The pressure variations induce bending in reinforced concrete silos, which can cause cracking. In steel silos, they can induce high compressive stresses which can significantly reduce the buckling strength.

The deviations from the Janssen pressures have been attributed to several factors including the inhomogeneity of the stored solids, the variation of wall roughness and the presence of small geometric imperfections in the silo wall (Jenike *et al.*, 1973a; Nielsen, 1983; Hartlen *et al.*, 1984; Ooi *et al.*, 1990). In particular, the unevenness of the internal surface of the silo wall (the wall geometric imperfections) is thought to be capable of inducing large local changes in wall pressure. The effects of "induced" local imperfection produced by mounting a pressure cell have been studied in detail by Askegaard and his co-workers (Askegaard *et al.*, 1972; Askegaard and Andersen, 1982). Their experimental investigation found that small irregularities in the silo wall can give rise to considerable local variation of wall pressure. Some simple approximate calculations using rather restrictive assumptions have also been undertaken (e.g., Nilsson, 1986). However, no proper investigation of the effects of geometric imperfections appears to have been performed.

Geometric imperfections in practical silo structures are known to have a major effect in reducing the structural strength of metal silos (Rotter and Teng, 1989). However, these studies did not include the effects of geometric imperfections on the wall pressures and the corresponding stress changes in the silo wall. If a geometric imperfection changes the stresses in the wall significantly, this might increase or decrease the risk of structural failure. For metal silos, imperfections in the form of a circumferential weld depression are common and have been identified as the most damaging type of imperfection for axial compression buckling (Rotter and Teng, 1992). For concrete silos, the slip forming technique used in construction can also lead to a local ring imperfection in the wall. In this paper, an axisymmetric deviation is introduced into an initially unstressed perfectly cylindrical silo wall to simulate such a local imperfection.

This paper presents a finite element study of the effects of a local axisymmetric geometric imperfection on the pressures acting on circular silo walls. The effects of the geometry and height of imperfection are also explored.

## 2. THE FINITE ELEMENT ANALYSIS

### 2.1. *General*

There have been many attempts at finite element predictions of wall pressures on geometrically perfect silos (e.g. Bishara *et al.*, 1983; Mahmoud and Abdel-Sayed, 1981; Haussler and Eibl, 1984; Rombach and Eibl, 1989). These studies often involved complex characterisations of the stored solid involving many parameters whose significance is not easily understood. It has been shown that complex characterisation of the bulk solid is not necessary in many situations, including the filling condition, for the satisfactory prediction of silo wall pressures (Ooi and Rotter, 1989, 1990). However, a proper modelling of the frictional contact between the bulk solid and the wall is essential.

No finite element predictions of pressure in geometrically imperfect silos appears to have been published. The theories which suggest that a geometric imperfection in the silo wall should lead to locally higher or lower pressures all rely on the solid having a finite stiffness. Here the bulk solid is treated as homogeneous and linear elastic. This simple assumption allows the solid stiffness to be characterised in a manner which is easily understood, so that its effects on wall pressures in imperfect silos can be assessed. This study should thus provide a basis for understanding the predictions of analyses involving more complex material characterisations.

### 2.2. *The imperfection*

An axisymmetric geometric perturbation was introduced into an initially unstressed perfectly cylindrical silo wall to simulate a circumferential geometric imperfection. The departure from the perfect cylindrical shape is shown in Fig. 1 and is given by

$$\delta = \delta_o e^{-\pi|z-z_o|/n\lambda}\left[\cos\left(\frac{\pi|z-z_o|}{n\lambda}\right)+\sin\left(\frac{\pi|z-z_o|}{n\lambda}\right)\right] \tag{1}$$

where $\lambda$ is the shell meridional bending half wavelength and has a value of $2.44\sqrt{Rt}$; $\delta_o$

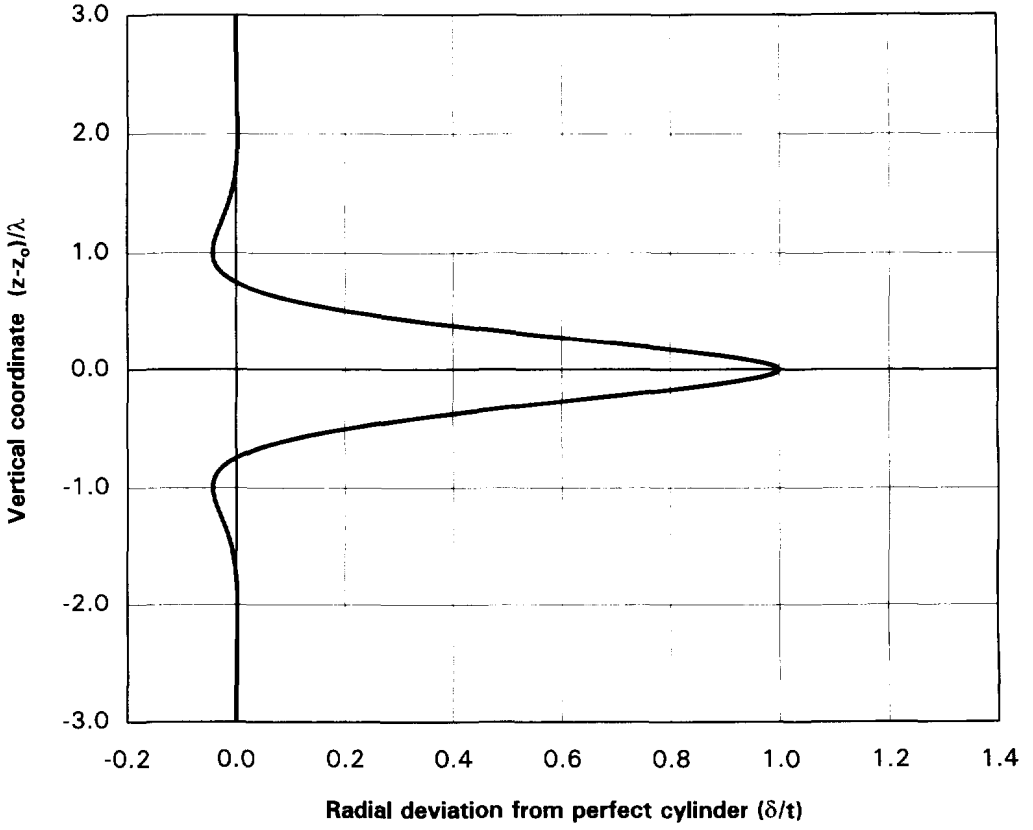


Fig. 1. Imperfection geometry.

and $z_0$ are the amplitude of the imperfection and the vertical coordinate of the centre of imperfection, respectively. The imperfection is applied in the inward radial direction (i.e. decreasing the silo cross-sectional area) as shown in Fig. 2. With this imperfection, the silo cross-sectional area increases slightly before reducing towards $\delta_0$ at the centre of the imperfection. This shape of geometric imperfection has previously been used in buckling analyses of silo walls (Rotter and Zhang, 1989; Teng and Rotter, 1992). The shape of the imperfection is closely related to the deformed shape which the wall would adopt if the imperfection were caused by weld shrinkage alone. Measurements of the imperfections in full scale silos indicate that the amplitude is typically of the order of 1–2 wall thicknesses (Ding, 1992; Coleman *et al.*, 1992).

2.3. *Finite element modelling*

A ground-supported cylindrical silo with a radius of 5 m, a height to radius ratio $H/R=2$ and a radius to wall thickness ratio $R/t=500$ was analysed (Fig. 2). For the stored solid, a conical surcharge angle of 25° (angle of repose) was used. The floor of the silo was treated as rough, providing a full horizontal restraint to the stored solid. The wall was assumed to be fixed at the base and free at the top. Young's modulus and Poisson's ratio of the silo wall were taken as $E_w=2\times10^5$ MPa and $\nu_w=0.30$, respectively, representing a steel wall. For the stored solid, Young's modulus and Poisson's ratio were taken as $E_s=10$ MPa and $\nu_s=0.30$, respectively.

The present investigation was carried out using the Abaqus finite element program (Hibbit *et al.*, 1993). A uniform body force was applied to the stored solid in the vertical downward direction to simulate gravity loading. An incremental loading approach was taken ignoring the effects of progressive filling. The axial symmetry of the silo and stored solids and a uniform loading allow the use of axisymmetric elements in the finite element modelling. An 8-node doubly curved continuum element (CAX8) and a 3-node quadratic shell element (SAX2) were used to model the stored solid and silo wall respectively. An example of the mesh is shown in Fig. 3. A classical Coulomb interface (ISL22A) was used

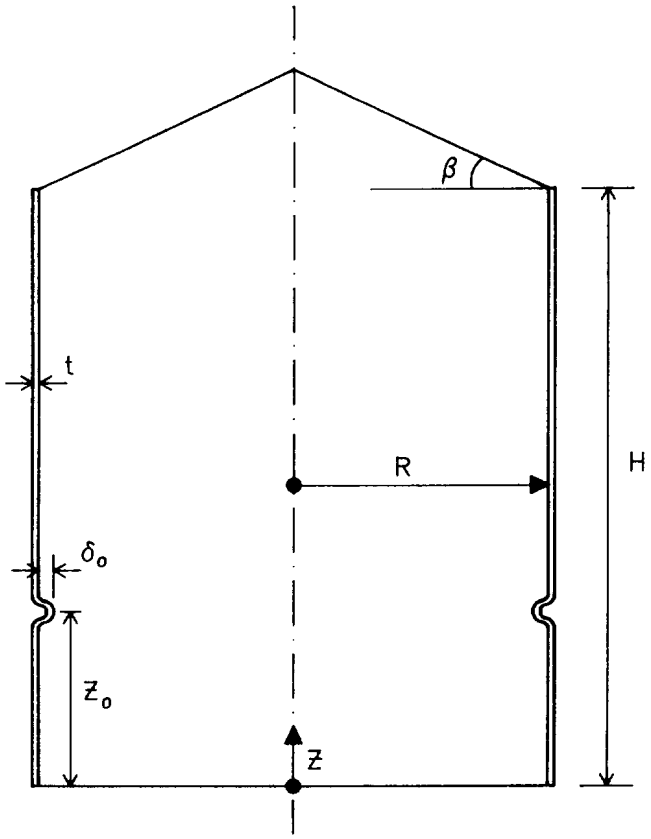


Fig. 2. Silo geometry.

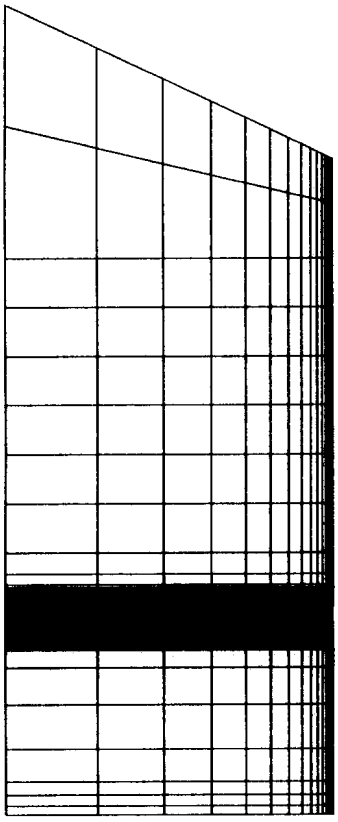

Fig. 3. Typical finite element mesh.

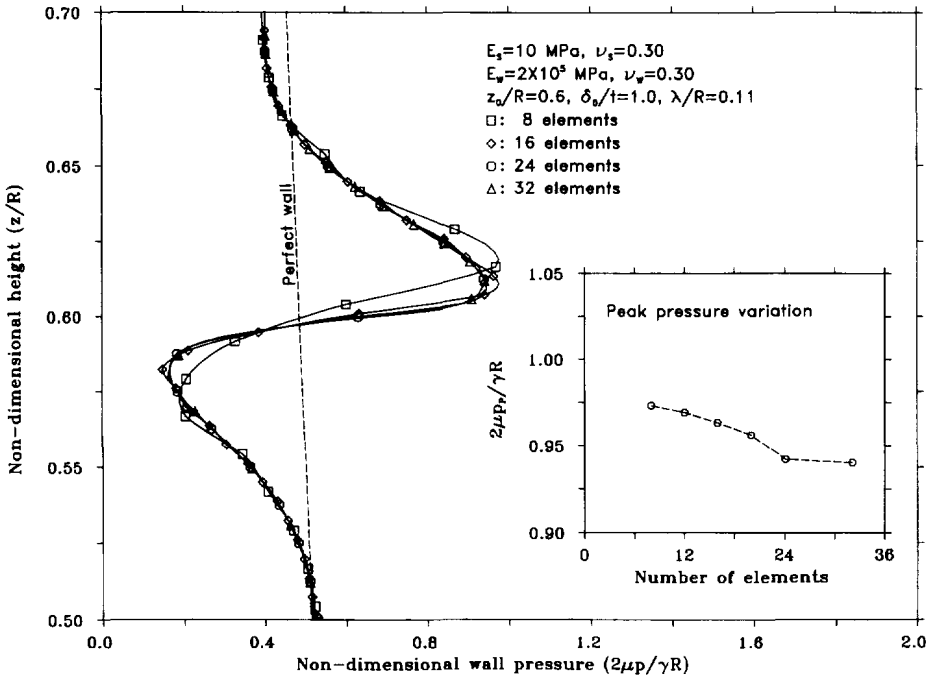


Fig. 4. Finite element mesh convergence study.

to model the frictional sliding between the solids and the shell. A wall friction coefficient of $\mu=0.50$ was used throughout. The elastic slip limit before sliding occurs was varied to investigate its effect. The results were almost completely independent of this parameter because all points slip except those very very close to the bottom of the silo. A value of $10^{-4}$ of the mean height of all the interface elements was set as the limit of the elastic slip for the present study.

### 2.4. *Convergence test*

The presence of the geometric imperfection causes rapid local changes in pressure. A finer element mesh is required in the area of the imperfection to obtain accurate predictions of wall pressure. However a very fine mesh may lead to computational instability, giving unrealistically high predicted wall pressures. To make sure that this does not happen and to check on the sensitivity of the results to the mesh, a convergence test was carried out by varying the number of elements over the height of the imperfection. The Gauss point stresses for four different meshes are shown in Fig. 4. The peak normal wall pressure induced by the local imperfection converges to a stable value. A stable and accurate prediction can be obtained using 24 elements over the zone $(z_0-\lambda)<z<(z_0+\lambda)$. It may also be noted that the position of the peak pressure moves slightly lower towards the centre of the imperfection as the number of elements is increased. For all the following analyses, a 24 element mesh over the imperfection zone was used.

## 3. JANSSEN PRESSURES

For a perfect silo with no geometric imperfection, the wall pressures are quite closely predicted by Janssen theory (1895) which is given by

$$p=\frac{\gamma R}{2\mu}[1-e^{-2\mu k(H-z)/R}] \tag{2}$$

in which $\gamma$ is the unit weight of the solid and the lateral pressure ratio $k$ is the ratio of normal wall pressure to mean vertical stress in the solid. The theory predicts that the normal wall pressure increases towards an asymptotic value at great depth ($p_z=\gamma R/2\mu$).

Janssen theory assumes a constant lateral pressure ratio $k$. Many methods for calculating the lateral pressure ratio have been proposed (e.g. Koenen, 1895; Jaky, 1948; Walker, 1966, Walters, 1973; Jenike *et al.*, 1973b; Hartlen *et al.*, 1984). The majority are based on the failure friction angle of the bulk solid. However, under storing conditions, it can be shown that much of the solid is not at failure (Ooi and Rotter, 1990), so the lateral pressure ratio $k$ can be approximated by the elastic value for a solid confined within an elastic shell (Ooi, 1990)

$$k = \frac{\nu}{1-\nu+\alpha} \tag{3}$$

in which $\alpha$ is the wall relative stiffness parameter and is equal to $E_s R/E_w t$. Janssen pressures form the basis for comparison with the finite element predictions in the next section.

## 4. TYPICAL SILO ANALYSIS

### 4.1. *General*

The typical squat silo outlined in Section 2 was analysed with and without an imperfection. The normal wall pressure distributions for both analyses are shown in Fig. 5. Janssen's prediction is also shown for comparison. The distribution for wall frictional traction is not shown here as it is similar to that for the normal wall pressure throughout the whole height, indicating that friction is fully mobilised everywhere for this silo.

### 4.2. *Perfect silo*

For the perfect silo, the finite element results agree very well with the Janssen solution except near the top and bottom boundaries (Fig. 5). Near the top, the Janssen pressures are much larger with a finite pressure at first wall contact which is clearly invalid. This is caused by taking the effective surface of the solid at $z=(H+R\tan\beta/3)$ to account for the conical surcharge above the solid/wall first contact (Fig. 2).

Near the bottom, the wall pressures are affected by the base boundary conditions. Towards the bottom, the wall pressure increases gradually to a peak value at around $z/R=0.2$. Below this peak, the finite element prediction shows a rapid decrease in pressure.

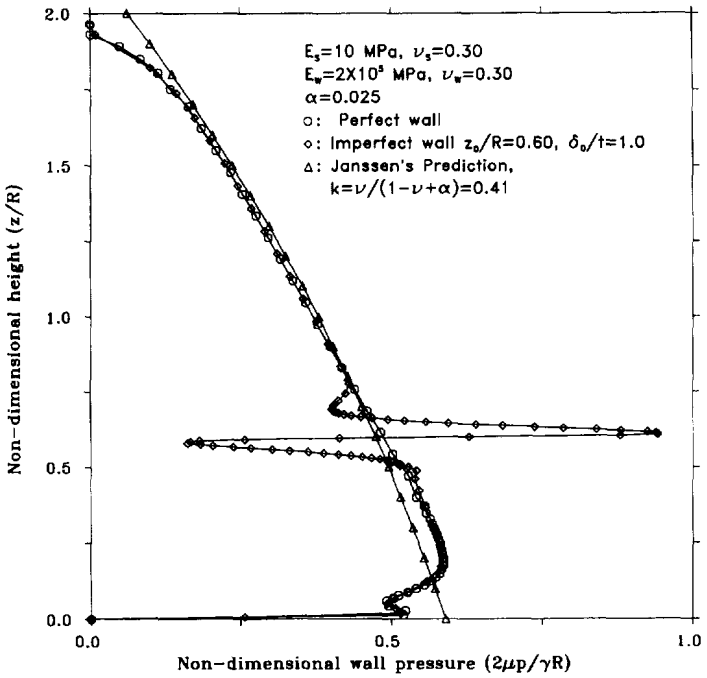


Fig. 5. Normal wall pressure for typical perfect and imperfect silo.

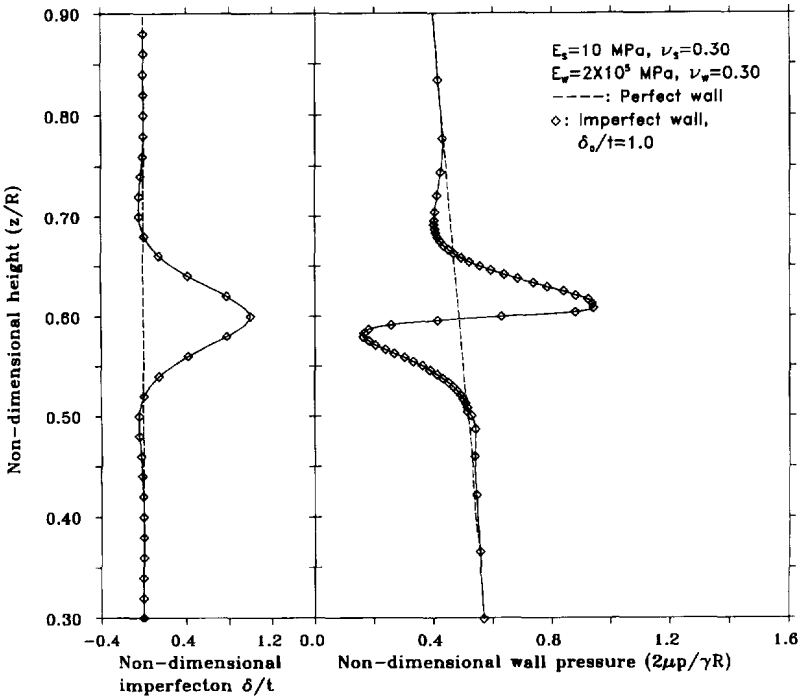


Fig. 6. Comparison on local pressure variation with imperfection geometry.

This phenomenon is not predicted by Janssen theory since it does not take into account the bottom boundary. It is caused by the vicinity of the silo floor and is affected somewhat by the modelling of the solid/floor interface. The shear stress in the solid caused by the floor restraint has greatly reduced the magnitude of the horizontal pressure near the wall, resulting in much smaller normal wall pressure.

Very close to the bottom of the wall ($z/R \approx 0.015$), another sharp and highly local peak can be seen. This is caused by the local wall bending phenomenon and solid/wall interaction. It is expected to be sensitive to the restraint condition of the silo wall but has no significant effects on the stresses in the wall and can therefore be ignored in design.

### 4.3. *Silo with an imperfection*

An axisymmetric geometric imperfection as described by eqn (1) was next introduced to the silo wall. It is located at $z_o/R = 0.6$ from the bottom and has an amplitude of $\delta_o/t = 1$.

A close up of the local pressure variation and the imperfection radial deviation with height are shown in Fig. 6. It is noted that pressure increases sharply to a peak value just above the centre of imperfection. On both sides of the increase, the pressures decrease below those for the perfect silo, with a much larger decrease on the lower side (Fig. 6). Away from the vicinity of the imperfection, the pressure distribution remains the same as that under a perfect wall condition.

This geometric imperfection has produced a rise in pressure from $0.49p_z$ to a maximum pressure of $0.98p_z$, which is an increase of 100% in normal pressure over that of a perfect silo. The two corresponding pressure drops are $0.06p_z$ and $0.36p_z$, respectively. It is possible that these two pressure drops are caused by the slightly larger silo cross-section at the two tails of the imperfection. This is further investigated in Section 5.

It appears that for every pressure increase caused by an imperfection, there are two corresponding pressure drops which tend to cancel out the overall increase in pressure for the whole silo. In other words, the present study suggests that axisymmetric geometric imperfection does not increase the overall Janssen pressures, but merely causes a redistribution of the pressures locally.

The wall meridional and hoop (circumferential) membrane stresses are shown in Fig. 7. The frictional traction of the solid against the wall generates axial compression in the silo wall. Since the pressure increase caused by the imperfection is bounded by two pressure

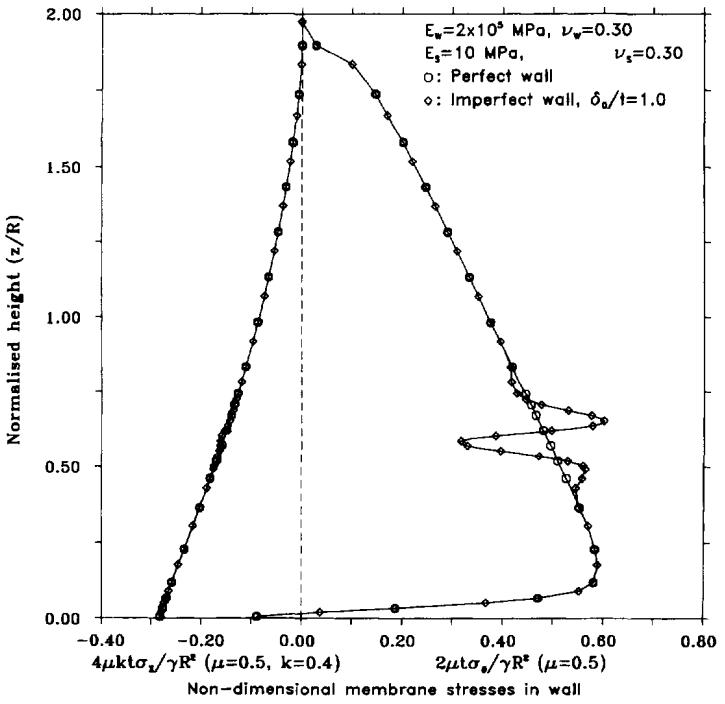


Fig. 7. Predicted circumferential and meridional membrane stresses in imperfect silo.

drops, the overall effects of the local traction variation on the wall meridional compression is minimal (Fig. 7). Away from the boundary and the geometric imperfection zone, the hoop stress differs from the normal wall pressure distribution only by the factor $R/t$ as would be predicted by the membrane theory of shells. Near the imperfection, the hoop stress is strongly affected by the changed geometry. The structural response spreads the effect of the local couple, leading to hoop tension above the imperfection and hoop compression below it. This is caused by the meridional membrane stress going over a local radially inward geometric imperfection, which has been studied extensively elsewhere (Rotter and Teng, 1989).

## 5. GEOMETRY OF LOCAL IMPERFECTION

It was thought that the slightly increasing silo cross-section associated with the tails of the reference imperfection could have caused the reduced pressure zones on both sides of the increased pressure zone (Fig. 5). Thus an alternative imperfection shape is chosen with a similar geometry but without the increasing radius in the tails of the imperfection. This modified imperfection is shown in Fig. 8 and is described by

$$\delta = \delta_o e^{-(\pi z/\lambda)^2} \tag{4}$$

Also shown in Fig. 8 is a close up view of the pressure distributions for both imperfections. The reduced pressure zones are clearly present for both geometric imperfections and are not caused by the slight increase in silo cross-section. The local pressure variations for both imperfections are almost identical since away from the tails, the geometries for both imperfections are very similar.

## 6. HEIGHT OF LOCAL IMPERFECTION

The effect of the height of imperfection is explored by comparing the results for two imperfections, described by eqn (1) with $n = 1$ and 2, respectively. The $n = 2$ imperfection has twice the height of the $n = 1$ imperfection (reference case). The imperfection shapes and a close up view of the resulting normal pressure distributions are shown in Fig. 9. The

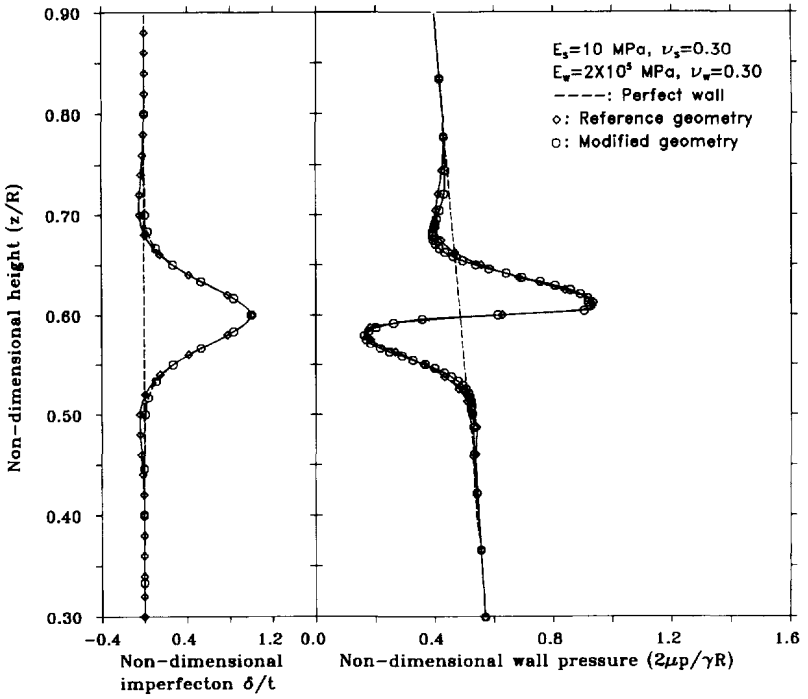


Fig. 8. Effect of imperfection geometry on pressure distribution.

local deviations in pressure have become smaller and spread over the increased height of the imperfection. The maximum increase in pressure has reduced from $0.49p_z$ to $0.11p_z$.

At the imperfection location, the solid is compressed radially as it consolidates and slips over the imperfection. As the compressive strain increases, the local rise in pressure is expected to increase accordingly. The average radial strains for these two imperfect silos are also shown in Fig. 9. Compressive strain is taken as positive here. The pressure deviations are seen to vary in a similar manner to the variation of the radial strains. However, the positions of the maximum pressure are much closer to the centre of the imperfections than

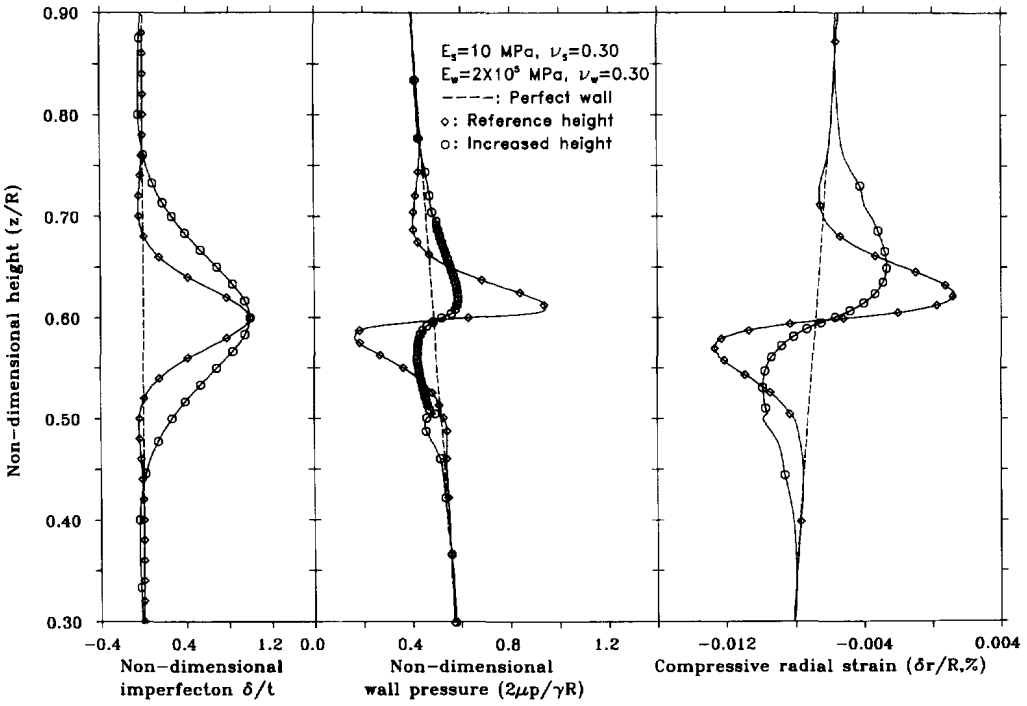


Fig. 9. Effect of imperfection height on pressure distribution.

the positions of the maximum compressive radial strain. Further study is required to understand this phenomenon.

For a silo, the degree of radial compression in the solid is strongly governed by the magnitude of slip against the wall locally. This, in turn, is affected by the stiffness of the solid and the flexibility of the wall. It should also be noted that if progressive filling is modelled, the magnitude of slip predicted would be smaller. This is because much of the settlement of the solid up to the height of the imperfection would have taken place before the solid reaches the imperfection without further filling. Therefore the pressures predicted in the present study are probably larger than what might have occurred. However the pattern of the local pressure changes due to the presence of a geometric wall imperfection is clearly illustrated.

## 7. EXPERIMENTAL EVIDENCE

A geometric wall imperfection has been suggested as a primary cause for the significant deviations from the Janssen pressure distribution observed in many experiments (Munch-Andersen and Nielsen, 1990; Ooi *et al.*, 1990; Ooi and Rotter, 1991). However, experimentally quantifying the effect of a geometric imperfection on silo wall pressures is difficult because the traditional method of measuring silo pressures is to use pressure cells, which are particularly difficult to install at locations with significant local geometric imperfection. The installation may also introduce a further "imperfection" in the wall (Askegaard *et al.*, 1972; Askegaard and Andersen, 1982). For thin metal silos, strain gauges have been used to infer the silo wall pressures (Blight, 1990; Bishara 1992; Rotter *et al.*, 1995). However, these silos are thin walled shells which exhibit complex behaviour, made even more complicated when geometric imperfections are involved. The strain readings must be subjected to careful analysis to infer the pressure distribution with confidence (Chen *et al.*, 1996).

Thus, proper experimental validation of the present theoretical study is not straightforward. However some limited evidence can be derived from published data. Figure 10 shows the pressures measured on a 152 mm diameter model silo by Jenike *et al.* (1973a) during flow. The measurements were made on a slightly converging and a slightly diverging cylinder, both with and without 'ledges ... of the order of magnitude of weld shrinkage at a typical girth seam' (Jenike *et al.*, 1973a). The result shows that wall pressures increased 'by a factor of two to three locally' at the imperfection. This compares with a factor of 2 for the reference case in the present theoretical study. Reduced pressure zones predicted in

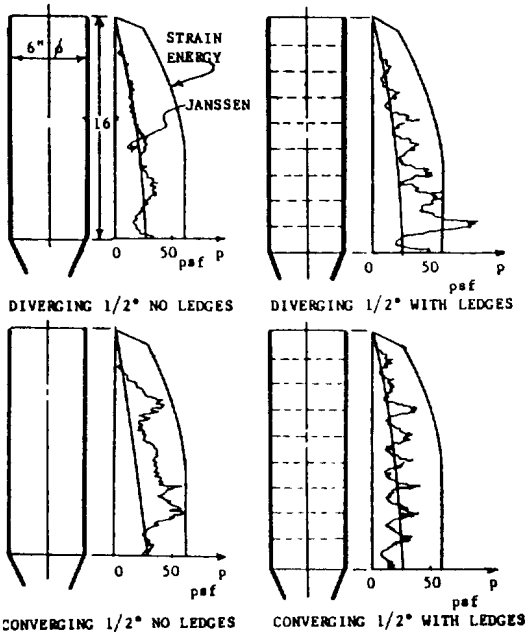


Fig. 10. Measured wall pressures in model silo with sand (after Jenike *et al.*, 1973a).

the present study were also found near the ledges in these tests (Fig. 10). Whilst these measurements were made during flow, it may be that consolidation of the stored solid during filling is sufficient to move the solid over the imperfection partially and induce the pressure changes. Similar deduction may be made from other experiments involving pressure cells after filling (Askergaard *et al.*, 1972).

The effect of an axisymmetric imperfection on silo pressures has been studied recently in a full scale experimental investigation (Rotter *et al.*, 1995). Initial analysis has shown that a considerable increase in pressure exists at the imperfection at the end of filling (Rotter *et al.*, 1995). However, this is beyond the scope of this paper and will be presented elsewhere.

## 8. CONCLUSION

A finite element study of the effects of an axisymmetric wall imperfection on pressures acting on circular silo walls has been presented. The presence of a geometric imperfection has been shown to cause significant local variation in wall pressures. A simple study exploring the effects of the geometry and height of imperfection has also been presented. The height of imperfection was found to affect the local pressure variation significantly. In general, the pressure deviations vary in a similar manner to the variation of the radial strains in the solid.

The present study has also shown that an axisymmetric geometric imperfection does not increase the overall wall pressures, but merely causes a redistribution of the pressures locally. The corresponding pressure drops tend to cancel out the increase in pressure above the centre of imperfection. This implies that wall imperfection has little effect on the meridional membrane stress in the silo wall.

## REFERENCES


Askegaard, V. and Andersen, E. Y. (1982). Consequence of loading history and mounting procedure on stress cell measuring error. In *Proc., Euromech* 157 *Colloquium: Quality of mechanical observations on particulate media*, Copenhagen, August, pp. A1–A7.

Askegaard, V., Bergholdt, M. and Nielsen, J. (1972). Problems in connection with pressure cell measurements in silos (in English). *Bygningsstatiske Meddeselser* **42**, 33–74.

Bishara, A. G. (1992). Moments and axial force in circular silo walls during eccentric discharge (test data versus finite element analysis results). In *Silos-Forschung und Praxis Tagung* '92, Karlsruhe, 8–9 October, pp. 41–50.

Bishara, A. G., Ayoub, S. F. and Mahdy, A. S. (1983). Static pressures in concrete circular silos storing granular materials. *ACI Journal* **80**, 210–216.

Blight, G. E. (1990). Defects in accepted methods of estimating design loading for silos. *Proceedings of the Institution of Civil Engineers Part* 1 **88**, 1015–1046.

Chen, J. F., Ooi, J. Y. and Rotter, J. M. (1996). A rigorous statistical technique for inferring circular silo wall pressures from wall strain measurements. *Engineering Structures* **18**, 321–331.

Clarke, M. J. and Rotter, J. M. (1988). A technique for the measurement of imperfections in prototype silos and tanks. *Research Report R565*, School of Civil and Mining Engineering, Uni. of Sydney.

Coleman, R., Ding, X. L. and Rotter, J. M. (1992). The measurement of imperfections in full-scale steel silos. In *Proc., 4th Int. Conf. Bulk Materials Storage Handling and Transptn*, I. E. Aust., Wollongong, June, pp. 467–472.

Ding, X. L. (1992) Precise engineering surveying—application to the measurement of large scale steel silos. PhD thesis, Uni. of Sydney, Australia.

Hartlen, J., Nielsen, J., Ljunggren, L., Martensson, G. and Wigram, S. (1984). The wall pressure in large grain silos. *Document D2*: 1984 Swedish Council for Building Research, Stockholm.

Haussler, U. and Eibl, J. (1984). Numerical investigations on discharging Silos. *Journal of Engineering Mechanics Division, ASCE* **110**, 957–971.

Hibbit, Karlsson and Sorensen. (1993). *ABAQUS User's Manual, Ver.* 5.2, Hibbit, Karlsson and Sorensen Inc., U.S.A.

Jaky, J. (1948). Pressures in silos. In *Proc., 2nd Int. Conf. Soil Mech. Found. Engng*, Rotterdam, 21–30 June, **1**, pp. 103–107

Janssen, H. A. (1895). Versuche uber getreidedruck in silozellen. *Zeitschrift des Vereines Deutscher Ingenieure* **39**, 1045–1049.

Jenike, A. W., Johanson, J. R. and Carson, J. W. (1973a). Bin loads—part 2: concepts. *Journal of Engineering for Industry, Transactions ASME* **95**, 1–5.

Jenike, A. W., Johanson, J. R. and Carson, J. W. (1973b). Bin loads—part 3: mass flow bins. *Journal of Engineering for Industry, Transactions ASME* **95**, 6–12.

Koenen, M. (1895). Berechnung des seitenund bodendricks in silos. *Zentralblatt Bauverwaltung* **16**, 446–449.

Mahmoud, A. A. and Abdel-Sayed, G. (1981). Loading on shallow cylindrical flexible grain bins. *Journal of Powder and Bulk Solids Technology* **5**, 12–19.

Munch-Andersen, J. and Nielsen, J. (1990). Pressures in slender grain silos. In *CHISA : 2nd European Symp. and Strain in Particulate Solids*, Prague, 26–31 August.
Nielsen, J. (1983). Load distribution in silos influenced by anisotropic grain behaviour. In *Proc., Int. Conf. Bulk Materials Storage Handling and Transptn*, I. E. Aust., Newcastle, August, pp. 226–230.
Nilsson, L. (1986). The effect of imperfections on the pressure in grain silos. *Bulk Solids Handling* **6,** 899–901.
Ooi, J. Y. (1990). Bulk solids behaviour and silo wall pressures. PhD thesis, Uni. of Sydney, Australia.
Ooi, J. Y. and Rotter, J. M. (1989). Elastic and plastic predictions of the storing pressures in conical hoppers. *Transactions of Mechanical Engineering, I. E. Aust.* **ME14,** 165–169.
Ooi, J. Y., Pham, L. and Rotter, J. M. (1990). Systematic and random features of measured pressures on full-scale silo walls. *Engineering Structures* **12,** 74–87.
Ooi, J. Y. and Rotter, J. M. (1990). Wall pressures in squat steel silos from finite element analysis. *Computers and Structures* **37,** 361–374
Ooi, J. Y. and Rotter, J. M. (1991). Measured pressures in full scale silos : a new understanding. In *Proc., Bulk 2000 : Bulk Material Handling—Towards the year 2000*, London, 29–31 October, pp. 195–200.
Rombach, G. and Eibl, J. (1989). Wall pressure in eccentric discharged silos. FIP/ISO TC98/SC3/WG5 on Loads due to Bulk Materials, *FIP/ISO paper No.* 20/89, Karlsruhe.
Rotter, J. M and Teng, J. G. (1989). Elastic stability of cylindrical shells with weld depressions. *Journal of Structural Engineering, ASCE* **115,** 1244–1263.
Rotter, J. M. and Zhang, Q. (1989). Elastic buckling of imperfect cylinders containing granular solids. *Research Report R589*, School of Civil and Mining Engng, Univ. of Sydney, Feb.
Rotter, J. M., Ooi, J. Y., Chen, J. F., Tiley, P. J., Mackintosh, I. and Bennett, F. R. (1995). *Flow Pattern Measurement in Full Scale Silos*, British Materials Handling Board Publication, London
Teng, J. G. and Rotter, J. M. (1992). Buckling of pressurized axisymmetrically imperfect cylinders under axial loads. *Journal of Engineering Mechanics ASCE* **118,** 229–247.
Walker, D. M. (1966). An approximate theory for pressure and arching in hoppers. *Chemical Engineering Science* **21,** 979–997.
Walters, J. K. (1973). A theoretical analysis of stresses in silos with vertical walls. *Chemical Engineering Science* **28,** 13–21.